

pubs.acs.org/JACS Article

3D Covalent Organic Framework as a Metastable Intermediate in the Formation of a Double-Stranded Helical Covalent Polymer

Lacey J. Wayment, Xubo Wang, Shaofeng Huang, Matthew S. McCoy, Hongxuan Chen, Yiming Hu, Yinghua Jin, Sandeep Sharma, and Wei Zhang*



Cite This: J. Am. Chem. Soc. 2023, 145, 15547-15552



ACCESS I

Metrics & More

Article Recommendations

Supporting Information

ABSTRACT: The design and development of intricate artificial architectures have been pursued for decades. Helical covalent polymer (HCP) was recently reported as an unexpected topology that consists of chiral 1D polymers assembled through weak hydrogen bonds from achiral building blocks. However, many questions remained about the formation, driving force, and the single-handedness observed in each crystal. In this work, we reveal a metastable, racemic, fully covalently cross-linked, 3D covalent organic framework (COF) as an intermediate in the early stage of polymerization, which slowly converts into single-handed HCP double helices through partial

Chiral 1D Polymer Racemic 3D Framework **Covalent Bonds** Covalent Bonds Supramolecular Assembly

fragmentation and self-sorting with the aid of a series of hydrogen bonding. Our work provides an intriguing example where weak noncovalent bonds serve as the determining factor of the overall product structure and facilitate the formation of a sophisticated polymeric architecture.

INTRODUCTION

Helices are an intriguing class of structural motifs that have been studied for decades, from the initial discovery of the double helices of DNA¹ to the development of novel helical foldamers (oligomers),^{2,3} small molecule assembly,⁴ and large polymers.^{5,6} Recently, we reported a single-crystal structure of 1D helical covalent polymer (HCP), which forms an extended network of mechanically entwined double helices held together by hydrogen bonding interactions. HCP was formed from 2,3,6,7,10,11-hexahydroxyltriphenylene (HHTP) with three pairs of reactive diols utilizing the dynamic spiroborate linkage. Interestingly, only two pairs of diols of each HHTP reacted to form helical strands, leaving one unreacted diol group. The HCP has several unique features such as a high degree of polymerization, aligned lithium ions in the channels of the double helices that allow for excellent directional lithium-ion conduction, and each single crystal domain has a single chirality, where the bulk sample is racemic.^{7,8} However, some fundamental questions remain to be answered: (1) What is the driving force for the helical structure formation through the conversion of only two pairs of diols to spiroborates and one unreacted? (2) Can we convert all three diols into spiroborates and obtain an open framework using a similar synthetic approach? (3) Is HCP a kinetically trapped state or the most thermodynamically favorable topology? (4) How does the chirality evolve?

Herein, we report a detailed study on the reaction progress of the HCP formation and reveal the intricate equilibrium between the HCP topology and a 3D covalent organic framework with srs topology (srs-COF) (Figure 1). We found

that either srs-COF or the 1D HCP polymer can be obtained as the major species by a meticulous selection of reaction conditions, yet the HCP topology is more thermodynamically favored. We also reveal the possible mechanism of the chirality evolution in the HCP, which involves pre-organization of racemic helical structures in srs-COF and further self-sorting to form the single-handed HCP structure. 9-12 Our study sheds light on how weak supramolecular interactions compete with covalent bond formation and exert a control on the eventual reaction pathway. We anticipate that many intriguing synthetic polymers with remarkable structural features resembling sophisticated biological macromolecules can be formed through deliberate incorporation of weak supramolecular interactions into the dynamic covalent polymerization process.

RESULTS AND DISCUSSION

Polymerization Study. The progress of the polymerization was monitored by PXRD to investigate the mechanism of the HCP formation through the condensation reaction of HHTP with trimethyl borate (B(OMe)₃) in the presence of lithium hydroxide (LiOH). At different time intervals, the reaction was quenched and washed with methanol and acetone to analyze the polymeric reaction mixture. After 12 h at 120

Received: May 7, 2023 Published: July 5, 2023





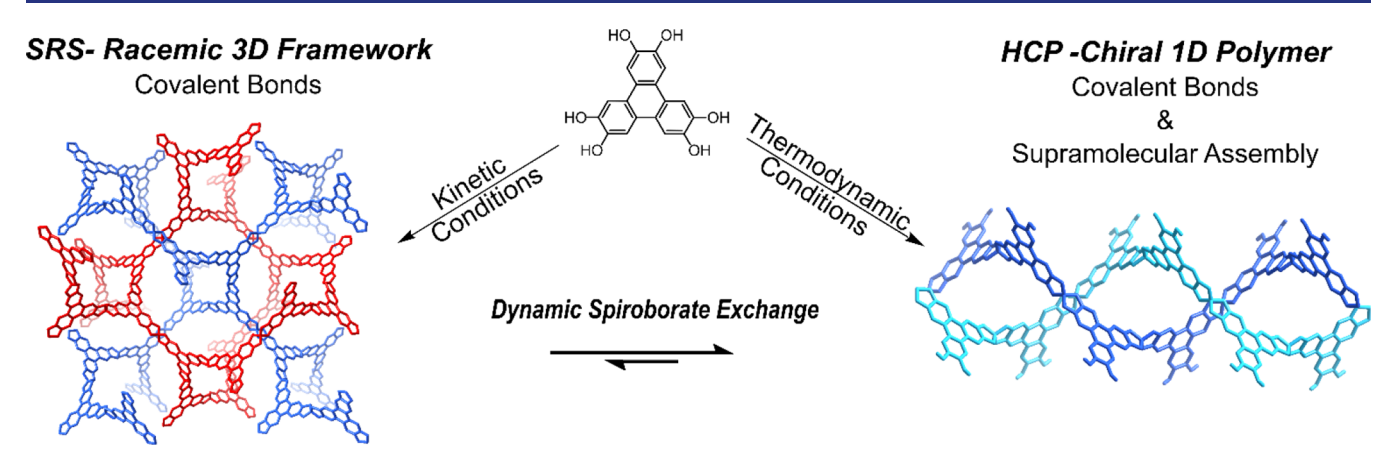


Figure 1. Illustration of srs-COF and HCP formation utilizing the dynamic spiroborate linkage. Kinetic conditions favor the formation of srs-COF while thermodynamic conditions favor HCP formation. srs-COF is a racemic framework connected with purely covalent bonds, whereas HCP is composed of 1D helical polymer chains with single-handedness (in each crystalline domain) that are assembled through hydrogen bonding interactions. The red and blue/light blue indicates opposite handedness and guest molecules are omitted from the structures for clarity.

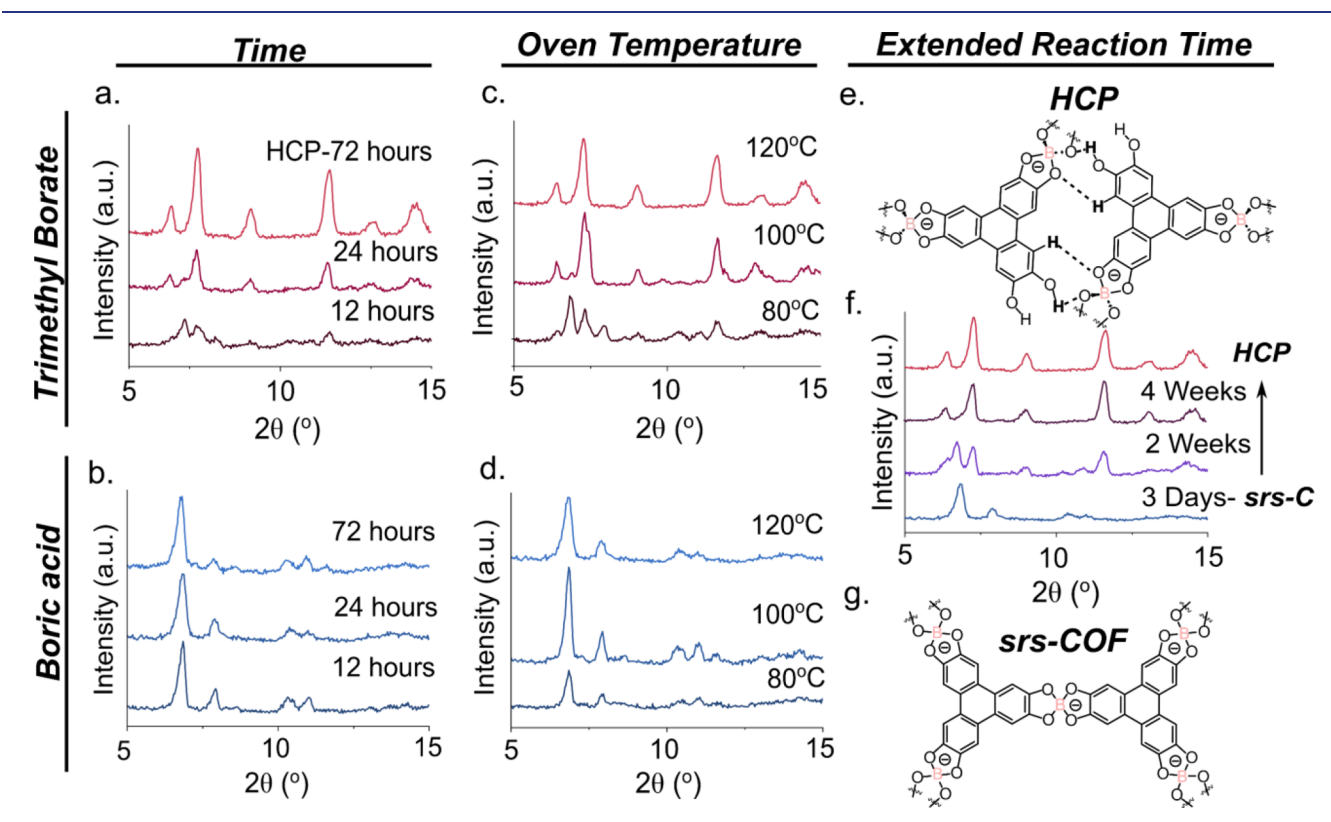


Figure 2. Experimental diffraction patterns of the polymers obtained when reaction times and oven temperatures were varied during spiroborate polymerization, using either trimethyl borate (a, c) or boric acid (b, d) as the boron reagent, respectively. Extending the reaction time of the spiroborate polymerization with boric acid resulted in the shift from srs-COF (g) to HCP (e) as the major phase after four weeks (f). The polymeric backbone of the structures is shown where the srs-COF backbone is built on purely covalent bonds (g) while HCP (e) is built on covalent and hydrogen bonds.

°C, there was a mixture of two phases, the HCP phase and a new unknown phase. However, by 24 h, HCP became the major species, and after approximately 3 days, the new phase was no longer present (Figure 2a). These results indicate that the new phase is a metastable intermediate and is only present at the early stage of the polymerization. We hypothesized that the new phase is likely an open framework structure where all three pairs of diols are fully reacted. To determine the structure of this new phase, we probed the reaction conditions, such as solvation of LiOH, boron reagent, water concentration,

temperature, and time, in the hope of forming the new phase predominantly.

Previously, the spiroborate polymerization was carried out by pre-stirring the reaction mixture at a lower temperature to dissolve LiOH, which acts as a base and deprotonates the diols and then heating the mixture in an oven without stirring to promote the growth and crystallization of the HCP. Using this synthetic approach, we observed that modulating the rate at which LiOH dissolves into solution is a key parameter for controlling the formation of the HCP crystals. To allow for

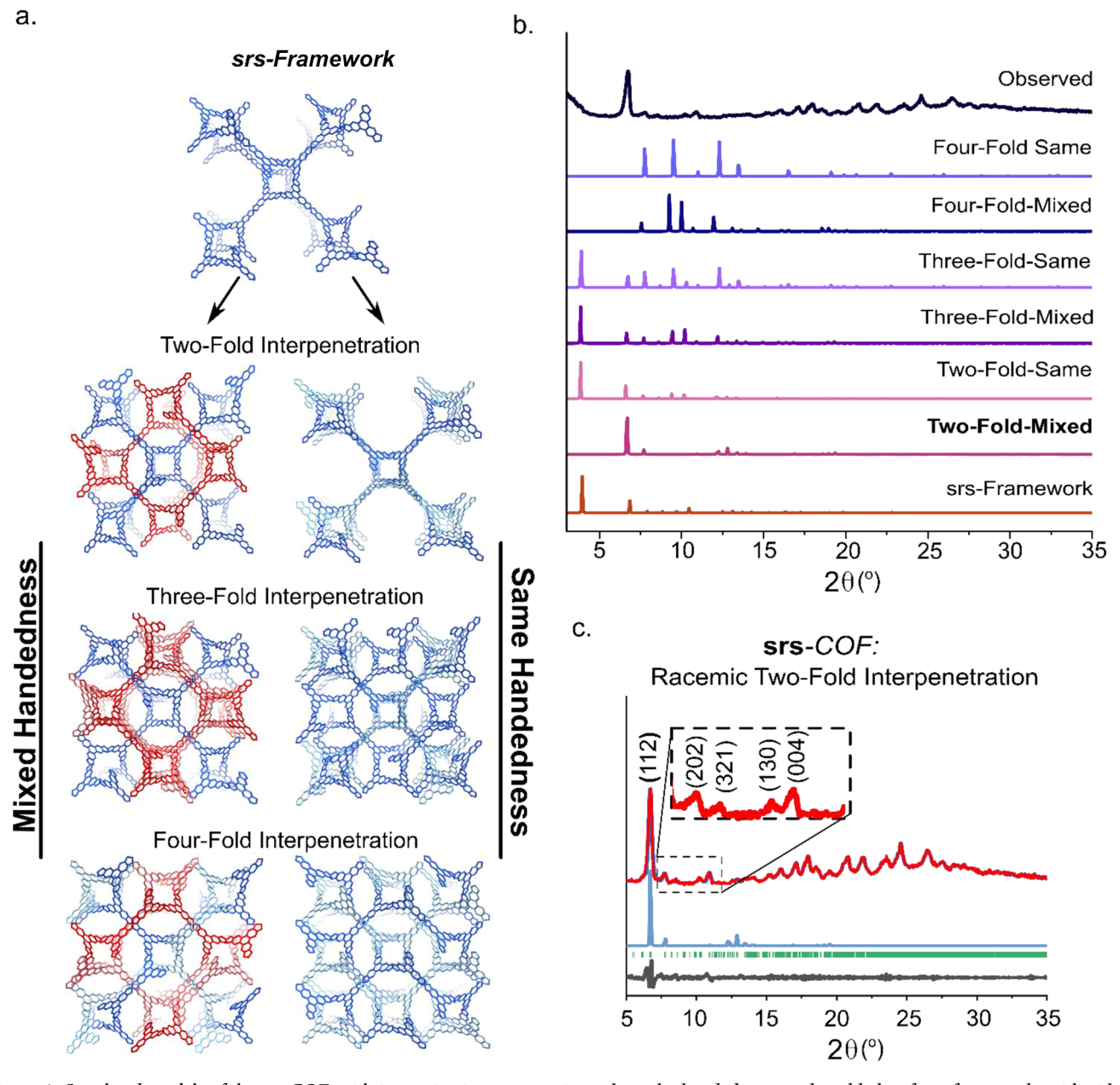


Figure 3. Simulated models of the srs-COF, with increasing interpenetration, where the handedness can be added to form frameworks with either all the same or mixed handedness. The red/pink and blue/light blue represents opposite handedness (a). The resulting diffraction patterns for the models show that only the two-fold interpenetration with mixed handedness matches the experimental pattern (b). Pawley refinement (dark blue) of the experimental data (red) with the simulation of the racemic two-fold interpenetrated (light blue), the difference between the simulation and experimental data (black), and the Bragg reflections are noted with green lines (c).

better solvation of LiOH and facilitate the reaction of diols with the boron reagent, initially, we attempted to incorporate more water in the reaction solution. However, although we observed the increase of the formation of the new phase with a higher content of water, the polymerization of HHTP with $B(OMe)_3$ consistently provided the HCP as the major species (Figure S1).

Interestingly, when we used boric acid $(B(OH)_3)$ instead of $B(OMe)_3$ as the boron source, the new phase became much more evident with new visible peaks at 6.72, 7.81, 10.22, and 10.90° (Figure S1). Additional water enhanced the formation of the new phase, but the phases became mixed, and the overall crystallinity diminished with excess water. We found it challenging to get an unequivocal new phase due to slight

shifts in the concentration of water that significantly affect the phase distribution when heating at 120 $^{\circ}$ C for 3 days.

Therefore, we next explored changing the temperatures and reaction time to better control the distribution of the phases. The effect of temperature on the phase distribution was studied in two ways: 1) the initial stir temperature was varied; 2) the oven temperature was varied. When the initial stir temperature was varied from 80 to 100 and 120 °C, we did not observe obvious change in the final phase distribution, indicating that the initial nuclei that form during the stirring step do not have a significant effect on the product distribution (Figure S2). When the initial stir temperature was kept the same (80 °C) and the oven reaction temperature was lowered to 80 °C, the reaction of HHTP with B(OH) $_3$ produced the

Right-handednesss All Right-Handed Right-handedness Slice and Self-sort' All Left-Handed Left-handedness

Figure 4. srs-COF and **HCP** architectures are built with helical components that have either left handedness or right handedness. However, the **srs-**COF structure is a racemic framework whereas **HCP** consists of 1D polymer chains where each crystalline domain has single handedness. We propose that the **srs-**COF will pre-organize the helices and provide helical oligomers that undergo a slice and self-sort transformation in order to be incorporated in the **HCP** topology.

new phase as the major phase (Figure 2d). The reaction of HHTP with B(OMe)₃ still produced a mixture of phases at 80 °C and HCP as the major phase at 100 °C (Figure 2c). Lowering the oven temperature during the polymerization process limits the reaction kinetics and the topological rearrangement, resulting in the formation of srs-COF as a kinetically trapped intermediate. The fact that the oven temperature, which influences the exchange, hydrolysis, and growth of the polymer phases, dictates the final phase distribution more significantly than the initial nucleation of the phases that further suggests that HCP is more thermodynamically favored and the new phase is only a metastable intermediate.

To intercept the polymerization at the COF stage, we quenched the reaction prematurely. As expected, the new phase was the only phase formed at shorter times (12 or 24 h) when using B(OH)₃ (Figure 2b). When the polymerization time with B(OH)₃ was extended past three days, the new srs-COF began to be converted to the HCP phase. After reacting for 2 weeks, a mixture of phases was present, and by 4 weeks, HCP was the only phase observed (Figure 2f). Although the HHTP polymerization kinetics and equilibrium heavily depend on the boron reagent, we observed that srs-COF will be gradually transformed to HCP with extended times and elevated temperatures. These results are consistent with our previous observation and further confirm that HCP is the thermodynamic topology.

Characterization of srs-COF. We isolated srs-COF by reacting HHTP, B(OH)₃, and LiOH under solvothermal conditions at 100 °C for 3 days and characterized it with FT-IR, NMR, PXRD, HR-TEM, and SEM to elucidate the structure. FT-IR spectra support the notion that the new phase is a spiroborate polymer, which shows a strong B-O stretch absorption at 1053 cm⁻¹ (Figure S3).^{7,13,14} The fingerprint region of the FT-IR spectrum shows only slight differences when compared to that of HCP and the OH stretch is attenuated as compared with HHTP (Figure S3). Solid-state ¹³C NMR spectra suggest that all three sides of HHTP are fully reacted as indicated by three symmetrical carbon signals. However, the broadening of the peaks implies that the polymerization in srs-COF is incomplete likely due to the difficulty of suppressing the HCP formation (Figure S4).

Similarly, the solid-state ¹¹B NMR (Figure S5) showed the presence of several boron species, which can be attributed to the relatively low polymerization degree and lower stability of srs-COF. However, the observed signals of boron species are consistent with those found in other recently reported materials.^{7,13,14} Meanwhile, the ⁷Li NMR spectrum (Figure S6) exhibited a dominant Li⁺ species that is in agreement with previous reports.^{7,14}

The SEM and HR-TEM analysis revealed a rodlike morphology of the srs-COF phase, which is notably different from the HCP single crystal morphology (Figures S7 and S8). In addition, the HR-TEM analysis also showed a lattice fringe with a d spacing of 1.3 nm that matches well with the $d_{(112)}$ and the electron diffraction pattern obtained from an orthorhombic crystal lattice (Figure S8). The PXRD demonstrates a clear structural difference between the phases (Figure 2f). We also compared the PXRD pattern to the starting materials (HHTP, LiOH, B(OH)₃) and confirmed that no major peaks are attributed to the starting materials (Figure S9). Based on the chemical characterization, it was evident that this new phase is a spiroborate polymer with a unique structure compared to HCP.

The spiroborate linkage contains a boron vertex that preferentially adopts a tetrahedral geometry. 13,15 However, the HCP single crystal structure demonstrates that the B-O bonds of the spiroborate are flexible and can adopt a strained dihedral angle of 66°. Thus, the new phase was anticipated to be a 3D COF with srs topology when considering the geometry of the HHTP and spiroborate. 16-19 Additionally, the spiroborate COF has the potential to display chirality since the extended structure consists of helices that can have either left or right handedness. Therefore, models of the COF with srs topology with either mixed or a single handedness were created and up to four-fold interpenetration was explored (Figure 3a). 20-22 The simulations of these models show the PXRD patterns of the new species match well with those of a racemic **srs** framework with the 2-fold interpenetration (Figure 3b). The major peaks at 6.72, 7.81, 8.55, 10.22, and 10.90° correspond to the (112), (202), (321), (130), and (004) planes. We determined the unit cell dimensions to be nearly cubic with a = 32.4043 Å, b = 32.3597 Å, and c = 31.8323 Åand a space group of PCA21 through Pawley refinement (RWP = 5.04% and RP = 3.12%) (Figure 3c).

Transformation of srs-COF into HCP. Although HCP crystals display single handedness in each crystalline domain, the intermediate in the polymerization is racemic srs-COF with a two-fold interpenetrated structure, as has been observed in other COF systems. 20,21 srs-COF and HCP are distinctly related because both contain helical components that have either right handedness or left handedness (Figure 4). In our previous work, we proposed that helical oligomers would initially form and subsequently become entwined as the hydrogen bonding interactions drove the formation of the HCP. However, in this work, we observed that the racemic srs-COF structure is present in the early stage of the polymerization and slowly converts to the HCP. Therefore, we propose that srs-COF is an intermediate species and contributes to the formation of the HCP in two ways: (1) preorganize the helices and (2) supply helical oligomers that will self-sort as the HCP crystals grow. The transformation requires the oligomers to undergo a partial hydrolysis (slice) and then self-sort into the correct orientation for the hydrogen bonding stabilization when condensing into the HCP structure. The thermodynamic favorability of HCP and srs-COF cannot be directly compared due to the difference in their compositions. However, the stoichiometric relationship between HHTP, HCP, and srs-COF can be used to find the effective energy difference for the spiroborate linkage within the two polymeric structures. First, we calculated the electronic energy of a known HHTP crystal structure, the HCP crystal structure, and the srs-COF crystal structure while optimizing the geometry using self-consistent charge density functional tight-binding (DFTB) theory. Then, the effective reaction energy per spiroborate unit was calculated for HCP and srs-COF by accounting for the number of HHTP monomers and spiroborate bonds within the respective unit cells. This calculation shows that the energy of spiroborate formation in the HCP structure is 36.8 kJ/mol lower than that in the srs-COF and supports the notion that the HCP is thermodynamically more favorable compared to srs-COF. The experimental and calculation results indicate that the hydrogen bonding interactions provide higher stabilization force compared to covalent spiroborate formation.

CONCLUSIONS

In summary, to understand the formation of the unexpectedly chiral HCP topology that consists of covalent and noncovalent bonds in the spiroborate polymerization, we investigated the mechanism by exploring the parameters such as time, water content, and temperature. We found the racemic srs-COF is formed as a metastable intermediate in the early stage of the polymerization but is transformed to the thermodynamically favored HCP. srs-COF is proposed to pre-organize the helical structures and supply helical oligomers that will self-sort to grow the HCP structure. Although an individual hydrogen bond is much weaker than a typical covalent bond, the combined effect of a series of hydrogen bonding interactions is nearly additive and could be a determining factor of a product's structure. The strategy of incorporating weak secondary interactions into the synthetic design of polymetric architectures will undoubtedly lead to novel structures and functions.

ASSOCIATED CONTENT

Supporting Information

The Supporting Information is available free of charge at https://pubs.acs.org/doi/10.1021/jacs.3c04734.

Synthetic methods; equilibrium studies; and FT-IR, NMR, PXRD, and other additional data (PDF)

AUTHOR INFORMATION

Corresponding Author

Wei Zhang — Department of Chemistry, University of Colorado Boulder, Boulder, Colorado 80309, United States; orcid.org/0000-0002-5491-1155; Email: wei.zhang@colorado.edu

Authors

Lacey J. Wayment — Department of Chemistry, University of Colorado Boulder, Boulder, Colorado 80309, United States Xubo Wang — Department of Chemistry, University of Colorado Boulder, Boulder, Colorado 80309, United States; orcid.org/0000-0003-3522-7435

Shaofeng Huang — Department of Chemistry, University of Colorado Boulder, Boulder, Colorado 80309, United States; orcid.org/0000-0002-2565-0005

Matthew S. McCoy — Department of Chemistry, University of Colorado Boulder, Boulder, Colorado 80309, United States Hongxuan Chen — Department of Chemistry, University of Colorado Boulder, Boulder, Colorado 80309, United States;

orcid.org/0000-0003-4075-247X

Yiming Hu — Department of Chemistry, University of Colorado Boulder, Boulder, Colorado 80309, United States; orcid.org/0000-0002-0684-4031

Yinghua Jin — Department of Chemistry, University of Colorado Boulder, Boulder, Colorado 80309, United States Sandeep Sharma — Department of Chemistry, University of Colorado Boulder, Boulder, Colorado 80309, United States; orcid.org/0000-0002-6598-8887

Complete contact information is available at: https://pubs.acs.org/10.1021/jacs.3c04734

Author Contributions

All authors have given approval to the final versions of the manuscript.

Funding

W.Z. thanks the support from National Science Foundation (Grant CHE-2108197). X.W. was supported through the National Science Foundation grant CHE-2145209. S.S. was supported by the grant from the Camille and Henry Dreyfus foundation. L.W. was supported by the Sewell Fellowship and the GAANN Fellowship.

Notes

The authors declare no competing financial interest.

ACKNOWLEDGMENTS

The authors thank Dr. Bimala Lama for the solid-state NMR measurements.

REFERENCES

- (1) Watson, J. D.; Crick, F. H. C. Molecular Structure of Nucleic Acids: A Structure for Deoxyribose Nucleic Acid. *Nature* **1953**, *171*, 737–738.
- (2) Hill, D. J.; Mio, M. J.; Prince, R. B.; Hughes, T. S.; Moore, J. S. A Field Guide to Foldamers. *Chem. Rev.* **2001**, *101*, 3893–4012.
- (3) Zhang, D.-W.; Zhao, X.; Hou, J.-L.; Li, Z.-T. Aromatic Amide Foldamers: Structures, Properties, and Functions. *Chem. Rev.* **2012**, *112*, 5271–5316.
- (4) Yashima, E.; Ousaka, N.; Taura, D.; Shimomura, K.; Ikai, T.; Maeda, K. Supramolecular Helical Systems: Helical Assemblies of

Small Molecules, Foldamers, and Polymers with Chiral Amplification and Their Functions. *Chem. Rev.* **2016**, *116*, 13752–13990.

- (5) Nakano, T.; Okamoto, Y. Synthetic Helical Polymers: Conformation and Function. *Chem. Rev.* **2001**, *101*, 4013–4038.
- (6) Yashima, E.; Maeda, K.; Iida, H.; Furusho, Y.; Nagai, K. Helical Polymers: Synthesis, Structures, and Functions. *Chem. Rev.* **2009**, *109*, 6102–6211.
- (7) Hu, Y.; Teat, S. J.; Gong, W.; Zhou, Z.; Jin, Y.; Chen, H.; Wu, J.; Cui, Y.; Jiang, T.; Cheng, X.; Zhang, W. Single crystals of mechanically entwined helical covalent polymers. *Nat. Chem.* **2021**, 13, 660–665.
- (8) Hu, Y.; Dunlap, N.; Long, H.; Chen, H.; Wayment, L. J.; Ortiz, M.; Jin, Y.; Nijamudheen, A.; Mendoza-Cortes Jose, L.; Lee, S.-H.; Zhang, W. Helical Covalent Polymers with Unidirectional Ion Channels as Single Lithium-Ion Conducting Electrolytes. *CCS Chem.* **2021**, *3*, 2762–2770.
- (9) Ji, Q.; Lirag, R. C.; Miljanić, O. Š. Kinetically controlled phenomena in dynamic combinatorial libraries. *Chem. Soc. Rev.* **2014**, 43, 1873–1884.
- (10) Safont-Sempere, M. M.; Fernández, G.; Würthner, F. Self-Sorting Phenomena in Complex Supramolecular Systems. *Chem. Rev.* **2011**, *111*, 5784–5814.
- (11) Liu, M.; Zhang, L.; Wang, T. Supramolecular Chirality in Self-Assembled Systems. *Chem. Rev.* **2015**, *115*, 7304–7397.
- (12) Jin, Y.; Zhang, W. Dynamic Covalent Chemistry: Principles, Reactions, and Applications; John Wiley and Sons, 2017.
- (13) Wang, X.; Bahri, M.; Fu, Z.; Little, M. A.; Liu, L.; Niu, H.; Browning, N. D.; Chong, S. Y.; Chen, L.; Ward, J. W.; Cooper, A. I. A Cubic3D Covalent Organic Framework with nbo Topology. *J. Am. Chem. Soc.* **2021**, *143*, 15011–15016.
- (14) Du, Y.; Yang, H.; Whiteley, J. M.; Wan, S.; Jin, Y.; Lee, S.-H.; Zhang, W. Ionic Covalent Organic Frameworks with Spiroborate Linkage. *Angew. Chem., Int. Ed.* **2016**, *55*, 1737–1741.
- (15) Downard, A.; Nieuwenhuyzen, M.; Seddon, K. R.; van den Berg, J.-A.; Schmidt, M. A.; Vaughan, J. F. S.; Welz-Biermann, U. Structural Features of Lithium Organoborates. *Cryst. Growth Des.* **2002**, *2*, 111–119.
- (16) O'Keeffe, M.; Peskov, M. A.; Ramsden, S. J.; Yaghi, O. M. The Reticular Chemistry Structure Resource (RCSR) Database of, and Symbols for Crystal Nets. Acc. Chem. Res. 2008, 41, 1782–1789.
- (17) Yaghi, O. M.; O'Keeffe, M.; Ockwig, N. W.; Chae, H. K.; Eddaoudi, M.; Kim, J. Reticular synthesis and the design of new materials. *Nature* **2003**, *423*, 705–714.
- (18) Kalmutzki, M. J.; Hanikel, N.; Yaghi, O. M. Secondary building units as the turning point in the development of the reticular chemistry of MOFs. *Sci. Adv.* **2018**, *4*, No. eaat9180.
- (19) Park, J.; Hinckley, A. C.; Huang, Z.; Chen, G.; Yakovenko, A. A.; Zou, X.; Bao, Z. High Thermopower in a Zn-Based 3D Semiconductive Metal—Organic Framework. *J. Am. Chem. Soc.* **2020**, *142*, 20531–20535.
- (20) Liu, Y.; Ma, Y.; Zhao, Y.; Sun, X.; Gándara, F.; Furukawa, H.; Liu, Z.; Zhu, H.; Zhu, C.; Suenaga, K.; Oleynikov, P.; Alshammari, A. S.; Zhang, X.; Terasaki, O.; Yaghi, O. M. Weaving of organic threads into a crystalline covalent organic framework. *Science* **2016**, *351*, 365–369.
- (21) Yahiaoui, O.; Fitch, A. N.; Hoffmann, F.; Fröba, M.; Thomas, A.; Roeser, J. 3D Anionic Silicate Covalent Organic Framework with srs Topology. *J. Am. Chem. Soc.* **2018**, *140*, 5330–5333.
- (22) Han, X.; Yuan, C.; Hou, B.; Liu, L.; Li, H.; Liu, Y.; Cui, Y. Chiral covalent organic frameworks: design, synthesis, and property. *Chem. Soc. Rev.* **2020**, *49*, 6248–6272.

☐ Recommended by ACS

Crystallization of Dimensional Isomers in Covalent Organic Frameworks

Bo Gui, Cheng Wang, et al.

MAY 11, 2023

JOURNAL OF THE AMERICAN CHEMICAL SOCIETY

READ 🗹

Construction of Crystalline Nitrone-Linked Covalent Organic Frameworks Via Kröhnke Oxidation

Fangyuan Kang, Qichun Zhang, et al.

JULY 07, 2023

JOURNAL OF THE AMERICAN CHEMICAL SOCIETY

READ 🗹

Topological Isomerism in Three-Dimensional Covalent Organic Frameworks

Yaozu Liu, Qianrong Fang, et al.

APRIL 18, 2023

JOURNAL OF THE AMERICAN CHEMICAL SOCIETY

READ 🗹

Coordination Sphere Flexibility Leads to Elastic Deformation in a One-Dimensional Coordination Polymer Crystal

Sajesh P. Thomas, Bo B. Iversen, et al.

MARCH 06, 2023

CHEMISTRY OF MATERIALS

READ **C**

Get More Suggestions >